

**CRYSTALLIZATION EFFECTS OF CARBON NANOTUBES IN
POLYAMIDE 12**

A Thesis
Presented to
The Academic Faculty

by

Rolfe Bradley Johnson

In Partial Fulfillment
of the Requirements for the Degree
Master of Polymers in the
School of Polymer, Textile, and Fiber Engineering

Georgia Institute of Technology
August 2010

**CRYSTALLIZATION EFFECTS OF CARBON NANOTUBES IN
POLYAMIDE 12**

Approved by:

Dr. Meisha Shofner, Advisor
School of Polymer, Textile and Fiber Engineering
Georgia Institute of Technology

Dr. David Bucknall
School of Polymer, Textile and Fiber Engineering
Georgia Institute of Technology

Dr. Yonathan Thio
School of Polymer, Textile and Fiber Engineering
Georgia Institute of Technology

Date Approved: May 21, 2010

ACKNOWLEDGEMENTS

This thesis was completed thanks to the help and guidance of my advisor, Dr. Meisha Shofner, who has helped me throughout this journey. I would also like to thank my group members, Michelle Schlea, Dr. Jasmeet Kaur, Dr. Xiaolan Hu, Ji Hoon Lee, and Jae Ik Choi for their help and consultation through my work. I would also like to thank my thesis committee members, Dr. David Bucknall and Dr. Yonathan Thio for their time and consideration and input in the completion of this thesis.

TABLE OF CONTENTS

	Page
ACKNOWLEDGEMENTS	iii
LIST OF TABLES	vi
LIST OF FIGURES	vii
LIST OF SYMBOLS AND ABBREVIATIONS	viii
SUMMARY	ix
 <u>CHAPTER</u>	
1 Introduction	1
1.1 Nanocomposites	1
1.2 Carbon Nanotubes	3
1.3 Polyamides	6
2 Carbon Nanotube Weight Loadings	11
2.1 Materials	11
2.2 Processing	11
2.3 Characterization	13
2.4 Results	14
2.5 Conclusions	22
3 Carbon Nanotube Sizes	23
3.1 Materials and Processing	23
3.2 Results	24
3.3 Conclusions	28
4 Conclusions	30
4.1 Chapter 2 Conclusions	30

4.2 Chapter 3 Conclusions	30
4.3 Overall Conclusions	31
4.4 Future Work	32
APPENDIX: Peak Fitting Data	34
REFERENCES	36

LIST OF TABLES

	Page
Table 2.1: DSC Peak Splitting Crystallinity (Weight Loading)	19
Table 2.2: DSC Peak Parameter Positions (Weight Loading)	20
Table 2.3: DSC Overall Crystallinity (Weight Loading)	21
Table 3.1: DSC Peak Splitting Crystallinity (Size Comparison)	26
Table 3.2: DSC Peak Parameter Positions (Size Comparison)	27
Table 3.3: DSC Overall Crystallinity (Size Comparison)	28
Table A.1: DSC Peak Parameters (Weight Loading)	34
Table A.2: DSC Peak Parameters (Size Comparison)	35

LIST OF FIGURES

	Page
Figure 1.1: Nanocomposite Interface	3
Figure 2.1: Torque vs. Time Curve	12
Figure 2.2: First Cycle DSC Melting Peak (Weight Loading)	15
Figure 2.3: Second Cycle DSC Melting Peak (Weight Loading)	16
Figure 2.4: DSC Peak Fitting	17
Figure 3.1: Second Cycle DSC Melting Peak (Size Comparison)	25
Figure 4.1: γ' -phase Crystallinity as a Function of MWNT Concentration	32

LIST OF SYMBOLS AND ABBREVIATIONS

CNT	carbon nanotube
DSC	differential scanning calorimetry
SWNT	single-walled carbon nanotube
MWNT	multi-walled carbon nanotube
FWNT	few-walled carbon nanotube
MMT	montmorillonite clay
PP	polypropylene
PVA	poly(vinyl alcohol)
PVDF	poly(vinylidene fluoride)
DMSO	dimethyl sulfoxide
AFM	atomic force microscopy
SEM	scanning electron microscopy
TEM	transmission electron microscopy
XRD	x-ray diffraction
nm	nanometer
μm	micrometer
TPa	terapascal (10^{12} Pascals)
GPa	gigapascal (10^9 Pascals)
MPa	megapascal (10^6 Pascals)
wt. %	weight percent
rpm	revolutions per minute
mg	milligram

SUMMARY

Multi-walled carbon nanotubes (MWNTs) are a nanofiller that has desirable multifunctional properties. They have been shown to offer improved mechanical, thermal, and electrical properties in composites. Research has been studying their incorporation into polymer composites. Polyamide 12 is a polyamide of interest that has been manufactured to have lower moisture absorption and higher ductility than other commercial polyamides such as 6 and 6,6 at room temperature.

In these studies, MWNTs have been incorporated into polyamide 12 at different weight loadings and using MWNTs with differing outer diameters. The composites were melt processed and characterized using differential scanning calorimetry (DSC) to understand the effects of MWNTs on the crystallization behavior of polyamide 12. A melt peak splitting behavior was observed in the polyamide 12 and composite samples when the specimens were not allowed to fully anneal.

Total crystallinity in the samples remained the same between the polyamide 12 and composites when the samples were fully annealed. Total crystallinity increased by 1 to 4 percent in the composites over the polyamide 12 when samples were not fully annealed. The addition of MWNTs to the polyamide 12 system increased the amount of crystallization contained in the lower temperature melting peak. An increase in MWNT concentration resulted in an increase in the crystallinity contained in the lower temperature peak. The addition of smaller diameter MWNTs resulted in a further increase in the lower temperature peak when the outer diameter was below a critical size.

Chapter 1

The goal of the following research was to investigate the thermal behavior of carbon nanotubes (CNTs) in a polyamide 12 matrix. All composites were melt processed using the same conditions to minimize the influences of processing conditions. Processed samples were pressed into sheets through compression molding and annealed before differential scanning calorimetry (DSC). DSC studies were performed at four different cooling rates ranging between 10 °C/min and 40 °C/min to understand the effect of CNTs and the mechanics behind the behaviors. Two variables were studied independently to understand the effects of weight loadings and filler characteristic size, respectively. The experiments showed that the addition of CNTs affected the crystallization behavior of polyamide 12. Results showed that both the weight loadings and size had very distinct influences. The data showed that the crystallinity that occurred in the secondary shoulder peak increases as a function of the concentration of CNTs in the polyamide 12. The influences from the various sizes of CNTs used showed that the smaller diameter CNTs contribute more to the shoulder than the either of the larger diameter CNTs used at low cooling rates.

1.1 Nanocomposites

Polymer nanocomposites have been shown to offer property improvements that have not been seen with conventional filler composites.¹⁻² For the same volume loadings of fillers, nanocomposites have a higher percentage of interfacial area. This increase in interfacial area has been evidenced by Winey and Vaia³ where they compared different

filler shapes and characteristic sizes. This can be seen in Figure 1.1 where as you decrease the size of the filler, an increase in the relative area of interfacial polymer increases. Their graph shows the difference between fillers with low aspect ratios and high aspect ratios with spheres being in the middle. An assumption was made in the calculations by Winey and Vaia that the thickness of the interfacial area remained the same. Their calculations used an interfacial thickness of 6 nm which is on the order of the radius of gyration of a polymer. When the filler is on the nanometer scale, the amount of interfacial area can actually be more than the filler loading. Their calculations compared a 1 μm and 1 nm spherical particle and showed that the amount of interfacial area between the particles and polymer as well as the number of particles increases by six and nine orders of magnitude, respectively. The polymer interfacial area has been characterized to have different properties than the bulk matrix.⁴ With the introduction of this new polymer region, researchers have been able to use lower weight loadings of nanofillers than have previously been used for conventional composites.⁵

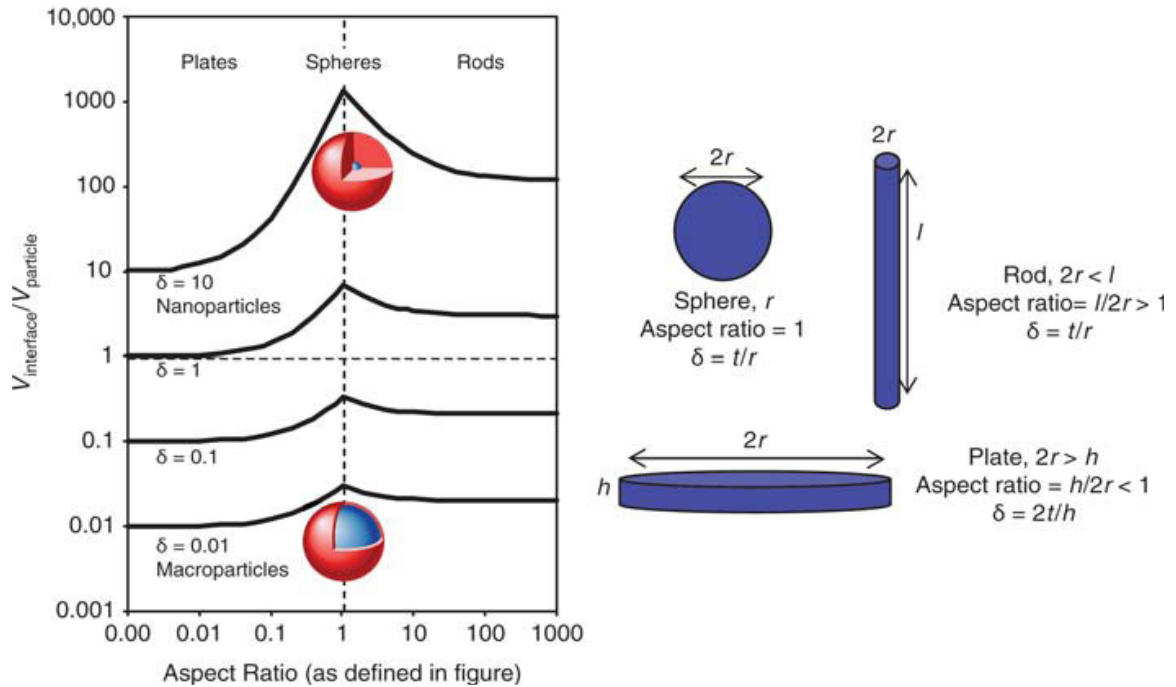


Figure 1.1: A schematic showing the relative differences in the percentage of interfacial area. At the nanoscale, the interfacial area makes up a bigger part of the composite at the same volume loading. From Winey and Vaia, MRS Bulletin, 2007.³

1.2 Carbon Nanotubes

In this thesis, the nanofillers of interest are CNTs. Following Iijima's widely cited paper in 1991,⁶ there has been overwhelming research concerning the properties and applications of CNTs. CNTs can generally be classified into two main types: single-walled carbon nanotubes (SWNTs) and multi-walled carbon nanotubes (MWNTs). CNTs have desirable multifunctional properties such as high mechanical properties, high electrical conductivity, and high thermal conductivity.⁷⁻⁸ These inherent properties have motivated research concerning CNTs in polymer matrix composites.

With some of the highest specific strengths and moduli known to date, CNTs have presented themselves as an excellent nanofiller.⁷ Treacy *et al.* showed an average modulus of 1.8 TPa for isolated MWNTs. Their studies showed a general trend in which

smaller diameter MWNTs exhibited higher moduli. Several groups have been able to perform tensile tests on isolated MWNTs.⁹ Yu *et al.* used a method involving two atomic force microscopy (AFM) cantilever tips inside of a scanning electron microscope (SEM). Upon testing the individual MWNTs, they found that the most common failure mechanism was pullout of the inner tubes. With their results, they calculated tensile strengths up to 63 GPa as well as tensile moduli as high as 950 GPa.

Many researchers have begun to study the use of CNTs in polymer composites as a filler. He *et al.*¹⁰ studied different concentrations of MWNTs in a poly(vinylidene fluoride) (PVDF) matrix. Their experiments focused mainly on the α -phase and β -phase crystallites. The α -phase crystallites are the most common in PVDF and characterized as alternating between trans and gauche configurations while the β -phase crystallites are characterized as an all trans configuration. They studied composites up to a concentration of 2.5 wt.% MWNTs in PVDF in steps of 0.5 wt.% MWNTs and observed that the percentage of β -phase crystallites in the samples increased as the concentration of MWNTs increased. Their DSC experiments also showed the appearance of a high temperature melting peak that increased in intensity as the MWNT concentration increased. Razavi-Nouri *et al.*¹¹ investigated the effects of SWNT concentration in polypropylene (PP). DSC experiments from Razavi-Nouri *et al.* showed an increase in the crystallization temperature with the addition of SWNTs. At their highest concentrations studied (1 and 2 wt.%), the crystallization temperature began to increase further over the neat PP up to a maximum of 11 °C. Their studies also showed that the addition of SWNTs into PP decreased the surface energy needed to form crystallites. This phenomenon resulted in an increase in the crystallization rate over the neat PP and

increased further with SWNT concentration. A study by Minus *et al.*¹² studied the crystallization effects of SWNTs in poly(vinyl alcohol) (PVA). They fabricated fibrils in a dimethyl sulfoxide (DMSO) solution and found that the addition of SWNTs at 1 wt.% to the system induced orientation. The neat PVA fibrils showed no orientation. The SWNTs increased the crystallization in the composite samples from 48% to 84%.

Few studies have been conducted regarding the effects of the diameter of CNTs on the properties of polymer nanocomposites. Zhang *et al.*¹³ investigated the effects of the size of MWNTs on the fatigue behavior in epoxies. They used four different diameters of MWNTs ranging between 5 nm and 70 nm and found interesting results. As the average diameter of the MWNTs decreased, the rate of crack propagation also decreased. This trend was attributed to the corresponding increase in MWNT number density in the sample. Their results also showed that MWNT length is more important than diameter when impeding crack propagation. Another study conducted by Giraldo *et al.*¹⁴ investigated the effects of two different diameters of MWNTs in polyamide 6. Their results showed that smaller diameter MWNTs improve the hardness in polyamide 6. Some DSC peak splitting was seen in their samples and they observed that the low temperature peak of the γ -phase crystallites shifted to a higher temperature in the MWNT composites. Giraldo *et al.* also reported that the interaction between smaller diameter MWNTs and polyamide 6 is stronger than that seen for the larger diameter MWNTs.

While polymers have a low tensile strength and electrical conductivity compared to metals and ceramics, the addition of CNTs into these types of systems works to improve these properties while maintaining a low cost.¹⁵ Liu *et al.*¹⁶ produced homogeneous composites and studied the crystallization behavior of MWNTs in

polyamide 6. Their neat polyamide 6 samples showed a double peak in DSC scans indicating both the γ -phase and α -phase crystallites being formed. In their MWNT composites, results show that the contribution from the γ -phase crystallites decreases and that there is a bigger contribution from the α -phase crystallites. With the α -phase crystallites exhibiting higher mechanical properties, Liu *et al.* propose that this could be a reason for the increases in yield strength and tensile modulus.

1.3 Polyamides

In the area of polymer nanocomposites, several groups have been investigating polyamide matrices for their use.^{1, 5} Polyamides are a wide class of polymers that have been used in many applications. Various polyamides have been used for purposes from everyday carpet to military parachutes. Chavarria and Paul investigated the effects of nanoclays on the mechanical properties of polyamide 6 and 6,6.¹⁷ They investigated both systems at 270 °C based on some torque experiments that showed that the melt viscosity of the polyamide 6 and 6,6 should be similar at that temperature. Using the same temperature for both systems was important in their studies to make sure that the organoclay experienced similar degradation during processing. By adding montmorillonite clay (MMT) to both systems, the yield strength and tensile modulus were enhanced. Chavarria and Paul saw larger increases in properties for the polyamide 6 given the same processing conditions as the polyamide 6,6 samples. Upon transmission electron microscopy (TEM) investigation, they found that the polyamide 6 composites had fully exfoliated structures while the polyamide 6,6 had a mixture of exfoliated and intercalated structures. Their results showed that the polyamide 6,6 had a higher degree

of crystallinity than the polyamide 6 which could influence the exfoliation behavior in the different polyamides. Polyamide 6 also retained its ductile nature at higher weight loadings of the nanoclay. At 270 °C with 4.9 wt% of montmorillonite clay, the modulus and yield strength of polyamide 6 were increased by 67% and 31%, respectively. For a 4.4 wt% montmorillonite clay sample of the polyamide 6,6 at 270 °C, the modulus was increased by 46% and the samples did not yield. Studying the same systems as Chavarria and Paul, Krause *et al.*¹⁸ saw similar comparisons regarding electrical conductivity using CNTs as the filler. In their studies, they varied mixing temperature, time, and speed to produce several sets of composites with CNTs mixed in both polyamide 6 and 6,6. Using light microscopy to characterize the macroscopic dispersion, they saw that longer mixing times and higher mixing speeds increased the overall dispersion. When mixing at their lowest speed (50 rpm), they saw that increasing the mixing time generally decreased the electrical resistivity of the CNT composites. However when they increased to higher mixing speeds (150, 200, and 300 rpm), an increase in mixing time resulted in an increase in electrical resistivity. This was attributed to the shortening of the CNTs. The higher mixing temperatures for both systems resulted in lower electrical resistivity. This was thought to be due to a better wetting of the CNTs from the lower viscosities of the polymer matrices.

Nanoparticle induced crystal phases have been observed in some polyamides. Wu and Liao¹⁹ studied the interaction between synthetic saponite and polyamide 6. They investigated two different concentrations (2.5 wt.% and 5 wt.%) of saponite in polyamide 6 through x-ray diffraction (XRD) and DSC. Upon quenching from the melt, the neat polyamide 6 showed XRD peaks from both the α -phase and γ -phase crystallites. The α -

phase crystallites are the thermodynamically stable form and are fully extended planar zigzag chains whereas the γ -phase crystallites are less stable and consist of pleated sheets held together through hydrogen bonding. When adding 2.5 wt.% saponite into the system, they found that this concentration preferred to form the thermodynamic α -phase crystallites. However when they increased the concentration to 5 wt.% saponite, the composite preferred to form the less stable γ -phase crystallites. Their studies showed that the crystal behavior was dependent on the nanoparticle content and the thermal history. In a different study by Lu *et al.*²⁰, nano-SiO₂ was investigated when incorporated into polyamide 6,6. Through DSC experiments, they observed a split melting peak that only occurred in the second heating cycle. At 1 and 3 wt.% nano-SiO₂, they saw the low temperature peak shift to higher temperatures as compared to the neat polyamide 6,6. Their studies also showed no change in the peak melting temperature between the neat and composite samples. Their studies did not characterize this peak splitting but mentioned that it could arise due to either a mixed crystal structure or melt-recrystallization. In this research the polymer of interest is polyamide 12. It is a polyamide that has been commercialized for its low moisture absorption as well as the ability to maintain higher degrees than polyamide 6 of ductility at low temperatures.²¹ It has a reported tensile strength and yield stress of 52.4 and 40.7 MPa at room temperature and 50% relative humidity, respectively. The tensile modulus is reported as 2200 MPa at the same conditions.

It has been observed by Sandler *et al.*²² that the addition of MWNTs to polyamide 12 alters the melting peak. Using the heating rate of 10 °C/min, their results showed no difference between the melting behavior of neat polyamide 12 and the MWNT

composites. However when the heating rate was increased to 30 °C/min, the neat polyamide 12 showed a low temperature melting peak that was not seen in the composites. They further investigated the changes and attributed the lack of low temperature peak in the composite samples to an exothermic deviation from the baseline. These results were independent of MWNT loading. Zhang *et al.*²³ studied the effects of a surface modified montmorillonite clay on the properties of polyamide 12. They reported that the addition of MMT increased both the yield strength and tensile modulus. They briefly discuss that the addition of MMT to the system changed the morphology from a spherulitic crystal form found in neat polyamide 12 into a lamellar form. In the MMT composites, the crystallites aligned along the surface of the clay particles. Their DSC curves showed evidence that the addition of MMT made the crystallization peak less broad and also shifted it to higher temperatures. One of their figures showed that the addition of MMT to the polyamide 12 introduced a low temperature peak in the system that was not discussed in detail.

Several groups have done further research into the crystallization behavior of polyamide 12.²⁴⁻²⁸ Northolt *et al.*²⁷ observed that there were monoclinic and triclinic structures in polyamide 12 in the early 1970s. They reported that the monoclinic form of polyamide 12 closely resembled the crystal structure found in polyamide 11 with the lateral spacing being within experimental error. Research has shown that four different crystal forms are present in polyamide 12: the γ -phase, γ' -phase, α -phase, and α' -phase. Of these, the γ -phase is the most common, thermodynamically stable form and characterized as a triclinic phase with a typical melting temperature of 179 °C.^{21, 24} Mathias and Johnson reported on the various ways to obtain the different crystal forms.²⁶

The γ' -phase has been characterized as also being triclinic in structure with a longer periodicity than that seen in the γ -phase and is obtained when the polyamide 12 sample is quenched from the melt and has a melting temperature of 175 °C.²⁹ Using DSC to observe the melting peaks, they report that the α -phase can only be obtained when the material is solution cast at low temperatures. The α -phase crystallites are characterized as being monoclinic in structure and having a melting temperature of 173 °C.²⁹ From their research, annealed samples only resulted in a melting peak that indicated that the γ -phase was present. Samples of polyamide 12 that were quenched from the melt showed indications of the γ' -phase being present. The α' -phase has been observed by Li *et al.*²⁴ They showed that this phase is only present at high temperatures and is present when the polyamide 12 is crystallized at 175 °C. When crystallized at a temperature close to the melting point such as this, the α' -phase is the most thermodynamically stable form. Later research by Ramesh²⁵ showed that upon cooling of the α' -phase to room temperature the crystallites transform into a γ -phase. The α' -phase has only been shown to exist at these elevated crystallization temperatures and disappears upon cooling. As of that publication, polyamide 12 is the only polyamide that showed this behavior. Other polyamides that have been shown to be in the α' -phase at elevated temperatures cool into an α -phase at room temperature.

Chapter 2

This chapter will discuss the experiments performed to understand the effect of different weight loadings of MWNTs on the crystallization behavior of polyamide 12. The size of the MWNTs and the processing conditions were kept constant during these experiments. DSC experiments showed that an increase in secondary peak contribution, referred to as γ' for the rest of this thesis, was seen with an increase in weight loadings.²⁶

2.1 Materials

DuraForm PA from 3D Systems was provided by Loughborough University for this research. It is a powder form polyamide 12 developed for selective laser sintering. MWNTs with outer diameters of approximately 12 nm from Thomas Swan, Inc. were provided by the High Performance Polymers and Composites (HiPPAC) Center at Clark Atlanta University. For this set of studies and following studies, these MWNTs will be referred to as the Elicarb MWNTs. Composites containing 0.2, 0.5, and 1 wt.% were prepared and characterized, and results were compared to those of the neat polymer.

2.2 Processing

The polyamide 12 was prepared by drying for 4 hours at 90 °C under vacuum before melt processing. All samples were processed at 190 °C in a laboratory scale batch mixer. A Brabender three-piece mixer was attached to an Intelli-Torque drive unit for processing. Roller blades were used to provide a high shear environment which is necessary to break up agglomerated CNT structures. All samples were mixed for 9

minutes at 75 rpm followed by mixing for 1 minute at 90 rpm. Nitrogen was flowed through the system during mixing to reduce degradation. All samples exhibited similar torque vs. time curves. As shown in Figure 2.1, there was an initial loading peak, corresponding to polymer melting, followed by a reduction in torque to a steady state value. All samples exhibited a small torque increase when the mixer speed was increased to 90 rpm. A stock temperature thermocouple was inserted into the system to accurately measure the temperature of each sample. The WinMix computer software was used to record the raw torque and temperature data provided by the machine. The data were further analyzed using Excel.

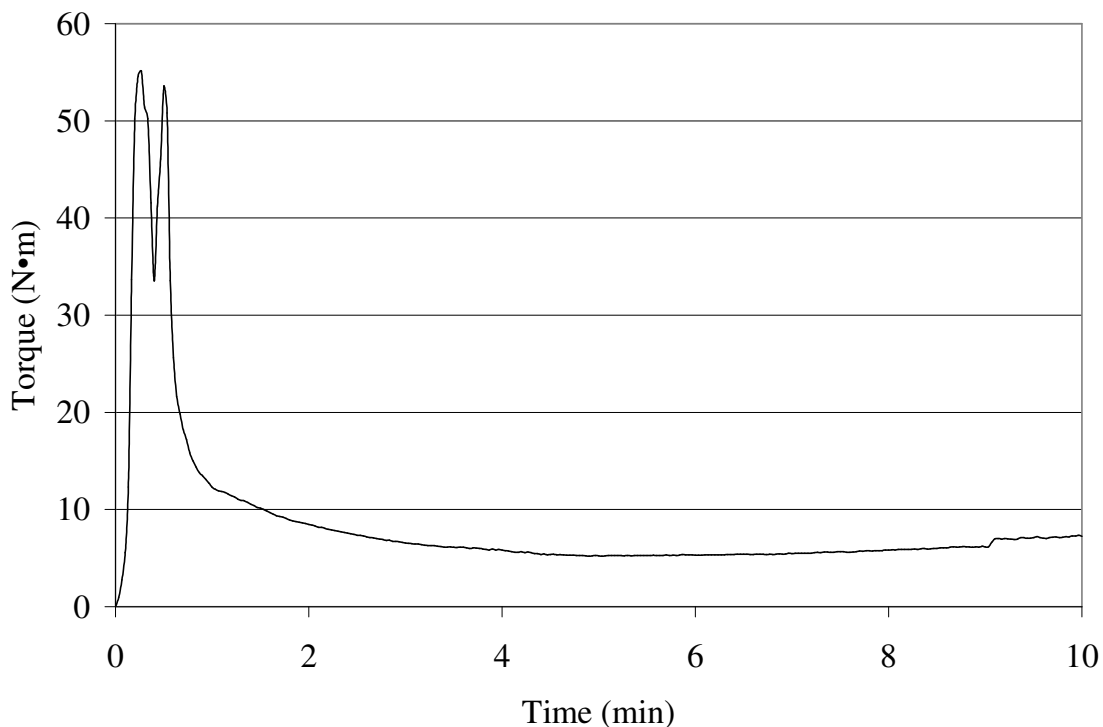


Figure 2.1: Torque vs. time curve of neat polyamide 12. The spike at the beginning is due to loading and initial melting which did not last past one minute in all samples. The increase in torque at 9 minutes is a result of an increase in the speed from 75 rpm to 90 rpm.

After melt processing, each sample was pressed into 6 x 6 inch sheets that were approximately 0.07 inches thick. This was done at 190 °C under a force of 4 tons for five minutes. The heat was turned off, and the samples were then allowed to cool slowly under pressure. The samples took approximately 5 hours to cool to room temperature. Linear calculations estimate this cooling rate to be around 0.5 °C/min. Prior to any type of characterization, all samples were annealed at 90 °C for 4 hours under vacuum. The samples were then allowed to condition for 40 hours at laboratory conditions according to the ASTM D 618 standard.

2.3 Characterization

DSC was performed using a TA Instruments Q200 DSC. Samples were measured out to be between 6.2 and 6.7 mg each. Samples were taken from different parts of the pressed sheets to get a good representation of the overall system. Four different cooling rates of 10 °C/min, 20 °C/min, 30 °C/min and 40 °C/min were used. Two trials of each sample at each cooling rate were run. These rates were used to determine the effect on cooling rate on the melting peak splitting upon second heating. The samples were first cooled to 0 °C then heated to 200 °C at 10 °C/min and held at 200 °C for 5 minutes. The samples were then cooled at one of the cooling rates mentioned above to 0 °C and held for 2 minutes. The samples were finally heated to 200 °C at 10 °C/min. Data were analyzed from both heating cycles to understand changes in polymer morphology due to the addition of MWNTs.

2.4 Results

The results showed that the addition of MWNTs do not significantly affect the overall crystallinity in the samples when the samples are allowed to fully anneal. Crystallinity values ranged between 27.8 and 29.1 % for the neat and composite samples. The neat sample had a crystallinity value of 28.2 %. There were not any significant changes in the melting temperature during both heating cycles for the neat and composite samples. The melting temperatures of the composites were within 1 °C of the neat material. The crystallization temperature increased between 5 and 8 °C in the MWNT composites over the neat polymer without a significant change between the composites. A similar effect with the crystallization temperature had been observed by Zhang *et al.*²³ when montmorillonite clay had been mixed with polyamide 12. Their samples also showed no change between the neat polyamide 12 and clay composites with regards to the melting temperature. With an increase in MWNT concentration, the melting peak contribution from the γ' -phase crystallites also increased. The γ' -phase contribution also decreased in percentage contribution at higher cooling rates.

When looking at the DSC curves between the neat and composite samples, the second heat data changed the most dramatically due to the accelerated cooling time from the melt as compared to the initial compression molding. The first and second heat data of the neat and composite samples can be seen in Figures 2.2 and 2.3. In Figures 2.2 and 2.3, the composite samples have been offset by an arbitrary amount for clarity. Each sample had a common melting peak that arises at approximately 178 °C due to the γ -phase crystallites. The neat sample has a clear separation in the melting peak upon second heating with a lower temperature melting peak appearing at approximately 172

°C. This peak was attributed to the γ' -phase crystallites of polyamide 12.²⁶ When the 0.2 wt.% of Elicarb MWNTs were added, the γ' -phase peak shifts to higher temperature (175 °C) and closer to the melting peak at ~178 °C. Giraldo *et al.*¹⁴ reported the same phenomenon with MWNTs in polyamide 6. In their case, the less stable crystal phase (γ) shifted towards the thermodynamically stable phase (α) while the peak temperature of the α -phase remained unchanged. This shift makes the γ' -phase crystallite contribution appear more as a shoulder to the melting peak as opposed to a separate peak. Comparisons between Figures 2.2 and 2.3 indicate that the cooling rate has an effect on the melting peak behavior. Further analysis was performed to understand these changes.

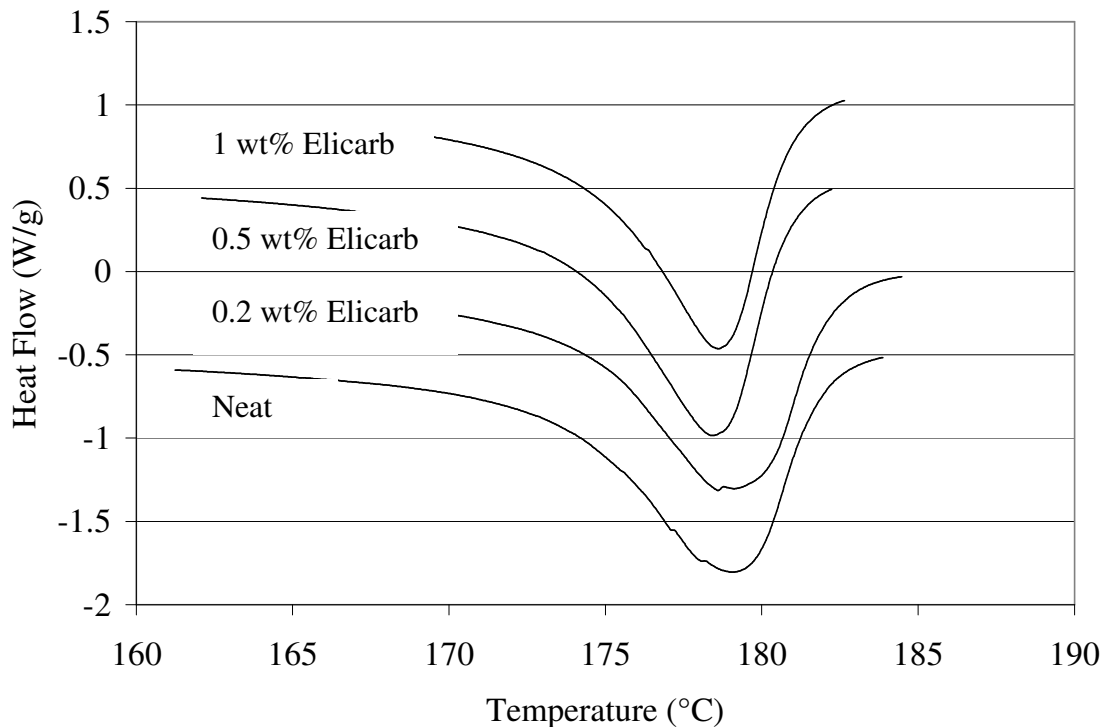


Figure 2.2: The neat polyamide 12 and composite samples upon initial heating. Note that there is not any significant peak splitting but there is a peak broadening in the neat material and low concentrations.

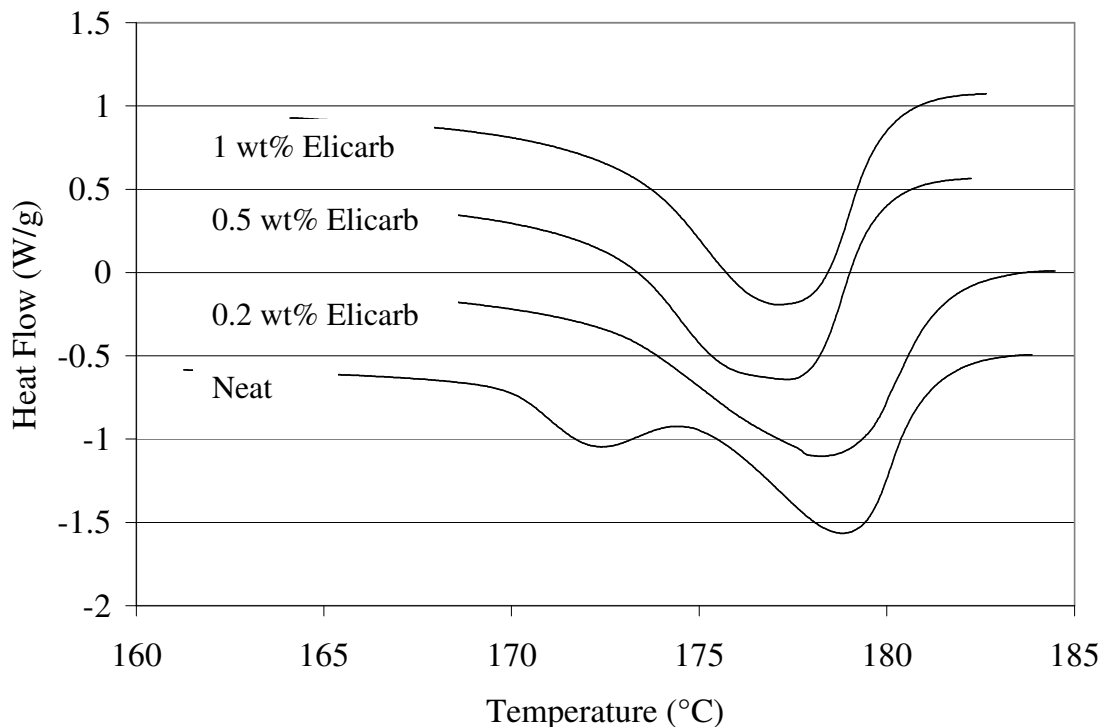


Figure 2.3: The neat polyamide 12 and composite samples upon second heating. At higher concentrations of MWNTs, the melting peak became one broad peak instead of two separate peaks.

Peak deconvolution was performed on the second heating cycle melting peaks to further quantify the differences between the neat polyamide 12 samples and the Elicarb MWNT composites. The peaks were fitted using two Gaussian peaks by minimizing the error. The area under the peaks was then converted into the percent crystallinity using the overall crystallinity obtained from the DSC. The raw data baseline was established from the point at which the derivative of the heat flow showed deviations on each end of the melting peak. Figure 2.4 shows an example of the data analysis done on one of the neat samples with a 10 °C/min cooling rate. The peak position, peak height, and peak width were all determined for each Gaussian peak. The first set of peaks on the neat polyamide 12 was chosen to best match the data and was further used as the starting point

for parameters for subsequent peak fitting. Altering all three parameters on each sample allowed for the best peak fitting and the temperature shifts that were seen in the γ' -phase peak. Peaks were fit to obtain the highest R^2 value for each curve. The minimum R^2 value obtained was 0.91 with most curves having an R^2 value greater than 0.95. A full listing of the peak parameters and R^2 values are listed in Tables A.1 and A.2.

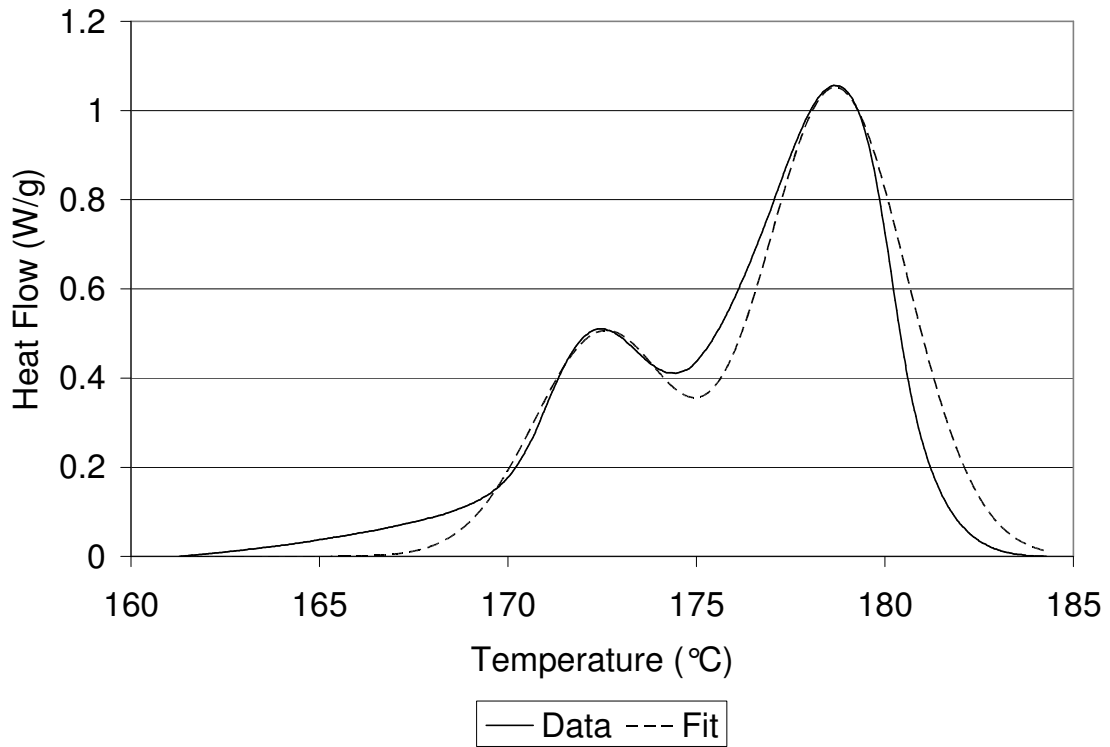


Figure 2.4: An inverted DSC curve of neat polyamide 12 analyzed using two Gaussian peaks. Peaks were fit by minimizing the error.

Comparisons between the neat polyamide 12 and the MWNT composites revealed insight as to their effects. When the cooling rate was increased, the contribution from the γ' -phase crystallites decreased in all cases. This trend can be observed best for the neat polyamide 12 samples where the γ' -phase crystallinity decreased from 7.0% to 2.5% when the cooling rate was increased. This indicated that an increase in the cooling rate

deterred the formation of the γ' -phase crystallites. A 3 to 5 percent crystallinity decrease was seen in the neat and composite samples, respectively. In all samples, there was a corresponding increase in the γ -phase crystallinity of approximately the same magnitude. The γ' -phase crystallinity values seen in the composite samples were larger than the neat polyamide and indicated a shift of the γ -phase to the γ' -phase crystallites in the composite samples. The amount of γ' -phase crystallites increased with the increasing MWNT concentration. However these increases in γ' -phase crystallites were not proportional to the increased amount of MWNTs added. The results from the increased cooling rates indicated that the cooling rate had the same effect on the neat polyamide as it did the composites. An increase in the concentration of MWNTs also increased the contribution from the γ' -phase crystallites. Table 2.1 lists the amount of crystallinity found in each crystalline phase.

Table 2.1: Peak splitting crystallinity for the second heating cycle arranged by concentration of MWNTs.

Filler	Cooling Rate	γ' -Phase Crystallinity %	γ -Phase Crystallinity %
Neat Polyamide 12	10 °C/min	7.0 ± 0.1	13.7 ± 0.1
	20 °C/min	5.4 ± 0.1	13.9 ± 0.1
	30 °C/min	3.8 ± 0.0	16.1 ± 0.0
	40 °C/min	2.5 ± 0.2	17.0 ± 0.2
0.2 wt% Elicarb	10 °C/min	10.4 ± 0.5	11.2 ± 0.5
	20 °C/min	9.3 ± 0.5	12.5 ± 0.5
	30 °C/min	9.5 ± 0.1	12.6 ± 0.1
	40 °C/min	7.2 ± 0.1	14.1 ± 0.1
0.5 wt% Elicarb	10 °C/min	13.4 ± 0.0	8.5 ± 0.0
	20 °C/min	9.9 ± 0.1	11.9 ± 0.1
	30 °C/min	11.1 ± 0.2	10.9 ± 0.2
	40 °C/min	8.5 ± 0.4	12.6 ± 0.4
1 wt% Elicarb	10 °C/min	14.1 ± 0.5	7.5 ± 0.5
	20 °C/min	11.3 ± 0.2	9.9 ± 0.2
	30 °C/min	11.2 ± 0.5	11.2 ± 0.5
	40 °C/min	9.9 ± 0.2	11.1 ± 0.2

The data listed in Table 2.2 details the center positions chosen for the Gaussian peaks of each sample. The data reveals that the peak position for the γ' -phase has a dependence on the cooling rate. As the cooling rate is increased from 10 °C/min to 40 °C/min, the γ' -phase peak shifts to a lower temperature. The γ -phase peak position shows no dependence on the cooling rate and has a 1 °C range between all samples. The remaining peak parameters and R^2 values are listed in Table A.1.

Table 2.2: Peak fitting positions for the second heating cycle arranged by concentration of MWNTs.

Filler	Cooling Rate	γ' position ($^{\circ}\text{C}$)	γ position ($^{\circ}\text{C}$)
Neat	10 $^{\circ}\text{C}/\text{min}$	172.5 ± 0.0	178.7 ± 0.0
	20 $^{\circ}\text{C}/\text{min}$	172.3 ± 0.2	179.2 ± 0.2
	30 $^{\circ}\text{C}/\text{min}$	170.8 ± 0.0	178.7 ± 0.1
	40 $^{\circ}\text{C}/\text{min}$	170.4 ± 0.1	178.8 ± 0.1
0.2 wt% Elicarb	10 $^{\circ}\text{C}/\text{min}$	175.1 ± 0.1	178.3 ± 0.1
	20 $^{\circ}\text{C}/\text{min}$	174.6 ± 0.1	178.9 ± 0.2
	30 $^{\circ}\text{C}/\text{min}$	173.7 ± 0.1	178.6 ± 0.0
	40 $^{\circ}\text{C}/\text{min}$	173.3 ± 0.2	178.3 ± 0.1
0.5 wt% Elicarb	10 $^{\circ}\text{C}/\text{min}$	175.7 ± 0.2	178.2 ± 0.2
	20 $^{\circ}\text{C}/\text{min}$	175.1 ± 0.1	179.1 ± 0.0
	30 $^{\circ}\text{C}/\text{min}$	175.0 ± 0.0	179.0 ± 0.1
	40 $^{\circ}\text{C}/\text{min}$	174.5 ± 0.3	179.0 ± 0.3
1 wt% Elicarb	10 $^{\circ}\text{C}/\text{min}$	176.1 ± 0.2	178.5 ± 0.4
	20 $^{\circ}\text{C}/\text{min}$	175.4 ± 0.0	178.6 ± 0.1
	30 $^{\circ}\text{C}/\text{min}$	175.3 ± 0.4	179.0 ± 0.7
	40 $^{\circ}\text{C}/\text{min}$	174.4 ± 0.0	178.4 ± 0.0

The crystallinity data showed overall similarities between the samples. Using the data from all eight samples at each concentration during the first heating cycle, the data showed that the crystallinity of the neat and composite polyamide 12 samples showed little to no change. As the results showed, the crystallinity of all samples was within experimental error. These results indicate that MWNT concentration has no significant effect on the crystallinity of the matrix when allowed to fully anneal. Looking at the second heating cycle in which the samples were not allowed to fully anneal, the crystallinity may increase slightly in the composite samples but it is not statistically significant. The crystallinity data can be seen in Table 2.3.

Table 2.3: Crystallinity data from the first and second heating cycles arranged by concentration of MWNTs.

Filler	Cooling Rate	1st Crystallinity %	2nd Crystallinity %
Neat Polyamide 12	10 °C/min	28.2 ± 1.4	20.7 ± 0.2
	20 °C/min		19.3 ± 0.9
	30 °C/min		19.9 ± 0.3
	40 °C/min		19.5 ± 0.2
0.2 wt% Elicarb	10 °C/min	27.8 ± 3.0	21.6 ± 0.3
	20 °C/min		21.7 ± 0.6
	30 °C/min		22.1 ± 0.1
	40 °C/min		21.3 ± 0.3
0.5 wt% Elicarb	10 °C/min	28.9 ± 1.1	21.8 ± 0.2
	20 °C/min		21.7 ± 0.1
	30 °C/min		22.0 ± 0.5
	40 °C/min		21.1 ± 0.2
1 wt% Elicarb	10 °C/min	29.1 ± 1.3	21.6 ± 0.6
	20 °C/min		21.2 ± 0.2
	30 °C/min		22.5 ± 0.2
	40 °C/min		21.1 ± 0.4

Through all of the samples and every cooling rate, the peak temperature of the melting peak did not change much. The average peak melting temperature across all samples was 178.4 °C with a standard deviation of 0.5 °C. Results showed that the addition and concentration of MWNTs influenced the crystal structure of polyamide 12. The γ' -phase peak increases significantly with the initial addition of MWNTs and continues to increase with further addition. Fully annealed polyamide 12 composite samples did not show a significant change in crystallinity from the neat polyamide 12. However when the cooling rate was increased and the samples were not allowed to anneal, the addition of MWNTs increased the overall crystallinity.

2.5 Conclusions

The results from the data showed that adding MWNTs to polyamide 12 can influence the crystal structure. When higher concentrations of MWNTs were added to the polyamide 12, a larger increase in the γ' -phase peak contribution was observed when the cooling rate was significantly high. Reports have shown that the γ' -phase crystallites have a longer periodicity than the γ -phase.³⁰ However this increase in the γ' -phase crystallinity does not account for the increase in MWNT concentration. These results could indicate that the 0.2 wt.% MWNT sample has the best dispersion. The data showed that the MWNTs do not significantly change the crystallization behavior of samples in which the material is allowed to fully anneal. The introduction of MWNTs maintains the amount of crystallinity at high cooling rates that is lost in the neat polyamide 12. Future work on this system should involve the investigation of higher weight loadings of MWNTs. These experiments would help understand if there is a limit to the amount of crystallization that occurs in the γ' -phase peak.

Chapter 3

This chapter will discuss the experiments performed to understand the effects of different size carbon nanotubes on the crystallization behavior of polyamide 12. The weight loadings and processing conditions were kept constant during these experiments. The smaller carbon nanotubes offered a larger increase in the γ' -phase peak percentage than the larger nanotubes. As seen in the MWNT concentration results in Chapter 2, smaller γ' -phase peak contributions were seen when the cooling rate was increased from 10 °C/min to 40 °C/min that corresponded with the amount of decrease seen in the neat polyamide samples. A similar result was also seen pertaining to the overall crystallinity in the second heating cycle. An increase between 1 and 4 percent crystallinity was seen and was not significantly influenced by the size of the nanotubes used.

3.1 Materials and Processing

The same polyamide 12 used in the previous experiments outlined in Chapter 2 was used for these experiments. Three different sizes of MWNTs were used for these experiments at a weight loading of 0.2 percent. This concentration was found to reduce the amount of agglomeration seen in the composites. Few-walled carbon nanotubes (FWNT) from XinNano Materials, Inc. with a diameter between 2 and 4 nm were donated for the research by Professor Otto Zhou. Larger MWNTs with a diameter ~50 nm were donated by the Center for Applied Energy Research (CAER) at the University of Kentucky. The Elicarb MWNTs used in Chapter 2 were used as the third size comparison. All MWNTs were unfunctionalized and used as received. All composites

were prepared by melt mixing, compression molding, and annealing as explained in Chapter 2. DSC experiments were performed using the same temperature program as described previously. Data were analyzed from both heating cycles to determine the effect of MWNT size in annealed samples and nonequilibrium samples.

3.2 Results

The results showed that the diameter of the MWNTs used in the composites has an effect on the crystallization behavior of polyamide 12. Analyzed data showed that the contribution from the γ' -phase peak in the composites was further enhanced by using smaller nanotubes at the 10 °C/min cooling rate. At the three higher cooling rates used, the size of the nanotubes became insignificant and showed similar results between the three size of nanotubes investigated. As was seen in Chapter 2 during the concentration studies, the first heat crystallinity value remained unchanged from the neat polyamide 12.

DSC data showed more significant changes between the FWNTs and the larger two sets of MWNTs used. This significant change is thought to be the result of a critical size scale where the polymer reacts differently to the nanotubes. Giraldo *et al.*¹⁴ reported similar observations in polyamide 6. They reported that a decrease in the MWNT diameter increased the interactions between polyamide 6 and the MWNTs. As shown in Figure 3.1, higher degrees of peak splitting can be observed as the size of the MWNTs decreases. Only the second heat data are shown for the differences as the first heat data looked very similar to what was observed in Chapter 2. The curves have been offset by an arbitrary amount for clarity. The FWNTs show the highest degree of splitting as seen in the bottom curve. They each have a common melting peak at approximately 178 °C

which can be attributed to the γ phase crystallites. The γ' -phase crystallites for these composites were centered at approximately 175 °C.²⁶

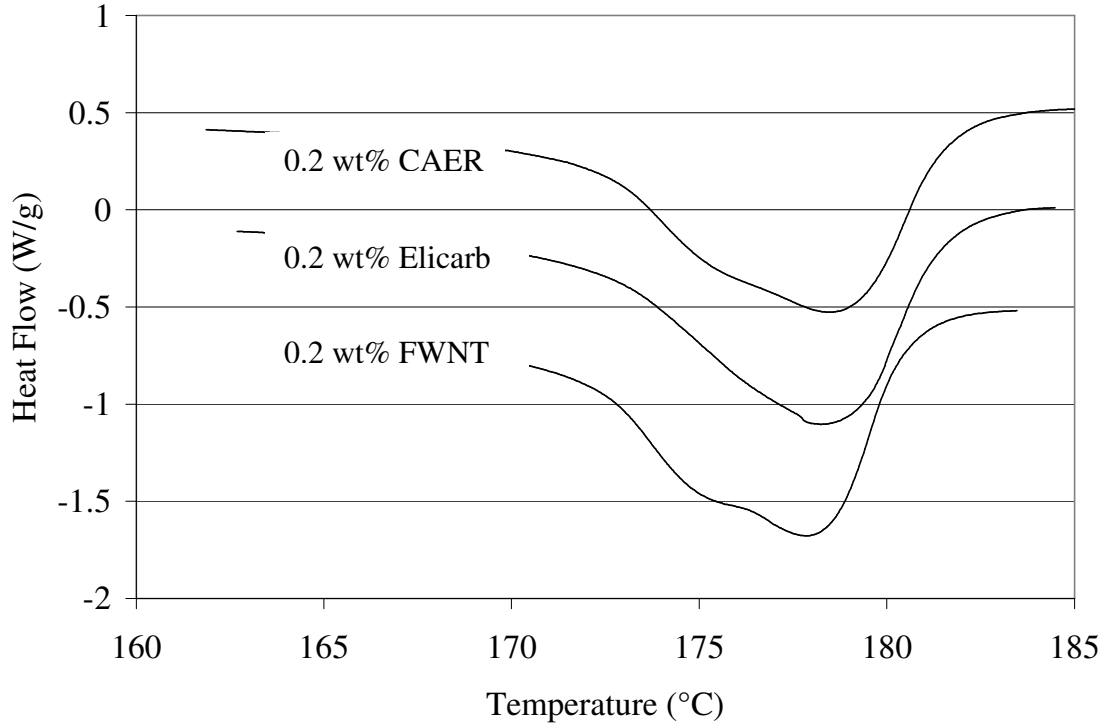


Figure 3.1: Second heat DSC data for the 0.2 wt% composites. The FWNT sample shows a larger γ' -phase peak. All γ' -phase peaks were centered at the same temperature within error.

Table 3.1 shows the peak splitting crystallinity data arranged by cooling rate. The smaller MWNTs showed more contribution in the γ' -phase peak when the 10 °C/min cooling rate was used. At the 10 °C/min cooling rate, the FWNT sample shows the largest change in γ' -phase peak contribution with an increase of 5.7 percent crystallinity. The Elicarb and CAER samples show smaller increases at 3.4 and 4.5 percent, respectively. When the cooling rate is increased to 20 °C/min, 30 °C/min, and 40

°C/min, the difference between the MWNT samples disappeared and was the same within experimental error.

These trends indicated that at the 10 °C/min cooling rate, the number of MWNTs seems to dominate the melting peak. While using smaller MWNTs, there is a higher absolute number of MWNTs in the sample for the same weight loadings of material. The smaller nanotubes therefore offer more nucleation sites assuming that the dispersions between the MWNT sizes did not change much. At the 10 °C/min cooling rate, the molten polymer is given enough time to flow and rearrange around the smaller MWNTs. When the cooling rate is increased to 20 °C/min, the size dependent effects disappeared from the samples.

Table 3.1: Peak splitting data for the second heating cycle arranged by size of MWNTs.

Filler	Cooling Rate	γ'-Phase Crystallinity %	γ-Phase Crystallinity %
Neat Polyamide 12	10 °C/min	7.0 ± 0.1	13.7 ± 0.1
	20 °C/min	5.4 ± 0.1	13.9 ± 0.1
	30 °C/min	3.8 ± 0.0	16.1 ± 0.0
	40 °C/min	2.5 ± 0.2	17.0 ± 0.2
0.2 wt% FWNT	10 °C/min	12.7 ± 0.0	9.1 ± 0.0
	20 °C/min	8.3 ± 0.9	13.0 ± 0.9
	30 °C/min	8.0 ± 0.1	13.5 ± 0.1
	40 °C/min	7.0 ± 0.3	14.7 ± 0.3
0.2 wt% Elicarb	10 °C/min	10.4 ± 0.5	11.2 ± 0.5
	20 °C/min	9.3 ± 0.5	12.5 ± 0.5
	30 °C/min	9.5 ± 0.1	12.6 ± 0.1
	40 °C/min	7.2 ± 0.1	14.1 ± 0.1
0.2 wt% CAER	10 °C/min	11.5 ± 0.4	11.0 ± 0.4
	20 °C/min	8.3 ± 0.1	14.3 ± 0.1
	30 °C/min	8.4 ± 0.9	13.6 ± 0.9
	40 °C/min	7.3 ± 0.0	13.9 ± 0.0

Table 3.2 details the center positions of the Gaussian peaks used. As was seen in Chapter 2, the positions of the γ' -phase peaks shift to lower temperatures as the cooling rate is increased. The neat polyamide 12 samples have the lowest γ' -phase peak positions and indicates results similar to what was seen by Giraldo *et al.*¹⁴ The γ -phase peaks remain relatively unchanged and only vary by 1 °C. The complete list of peak parameters along with the R^2 values are contained in Table A.2.

Table 3.2: Peak fitting positions for the second heating cycle arranged by size of MWNTs.

Filler	Cooling Rate	γ' position (°C)	γ position (°C)
Neat	10 °C/min	172.5 ± 0.0	178.7 ± 0.0
	20 °C/min	172.3 ± 0.2	179.2 ± 0.2
	30 °C/min	170.8 ± 0.0	178.7 ± 0.1
	40 °C/min	170.4 ± 0.1	178.8 ± 0.1
0.2 wt% FWNT	10 °C/min	175.3 ± 0.1	178.5 ± 0.1
	20 °C/min	174.6 ± 0.0	178.9 ± 0.3
	30 °C/min	173.5 ± 0.1	178.6 ± 0.0
	40 °C/min	172.9 ± 0.3	178.6 ± 0.1
0.2 wt% Elicarb	10 °C/min	175.1 ± 0.1	178.3 ± 0.1
	20 °C/min	174.6 ± 0.1	178.9 ± 0.2
	30 °C/min	173.7 ± 0.1	178.6 ± 0.0
	40 °C/min	173.3 ± 0.2	178.3 ± 0.1
0.2 wt% CAER	10 °C/min	175.4 ± 0.0	179.0 ± 0.0
	20 °C/min	174.4 ± 0.0	179.0 ± 0.1
	30 °C/min	173.3 ± 0.1	178.5 ± 0.1
	40 °C/min	172.6 ± 0.0	178.2 ± 0.0

The crystallinity data showed similarities between all samples. As was seen in Chapter 2, the fully annealed crystallinity in the neat polyamide 12 as well as the MWNT composite samples was the same when considering experimental error. Upon second heating of the samples, the crystallinity may have increased some in the composite samples, but it is not statistically significant. The data can be observed in Table 3.3.

Table 3.3: Crystallinity data from the first and second heating cycles arranged by concentration of MWNTs.

Filler	Cooling Rate	1st Crystallinity %	2nd Crystallinity %
Neat Polyamide 12	10 °C/min	28.2 ± 1.4	20.7 ± 0.2
	20 °C/min		19.3 ± 0.9
	30 °C/min		19.9 ± 0.3
	40 °C/min		19.5 ± 0.2
0.2 wt% FWNT	10 °C/min	28.9 ± 1.1	21.8 ± 0.2
	20 °C/min		21.2 ± 0.5
	30 °C/min		21.5 ± 0.2
	40 °C/min		21.7 ± 0.5
0.2 wt% Elicarb	10 °C/min	27.8 ± 3.0	21.6 ± 0.3
	20 °C/min		21.7 ± 0.6
	30 °C/min		22.1 ± 0.1
	40 °C/min		21.3 ± 0.3
0.2 wt% CAER	10 °C/min	28.5 ± 2.8	22.6 ± 0.7
	20 °C/min		22.6 ± 0.7
	30 °C/min		22.0 ± 0.2
	40 °C/min		21.2 ± 0.1

3.3 Conclusions

The addition of different sizes of MWNTs into polyamide 12 showed influences that are best observed at low cooling rates. At a cooling rate of 10 °C/min, the FWNT composites showed the largest increase in γ' -phase peak contribution while the Elicarb and CAER samples were not statistically different. This was attributed to the increased number of MWNTs present in the composite similar to the results of Zhang *et al.*¹³ on the crack propagation in epoxies. Even with the increased amount of MWNTs present in the FWNT composites, the changes in the crystallization does not account for the amount of extra MWNTs present in the samples. The nanotube ratios are approximately 1000 FWNT:70 Elicarb:1 CAER assuming the same length. These results could indicate that

the composites with larger MWNTs have better dispersion. On these size scales, the radius of curvature of the FWNTs could be impeding interactions with the polyamide 12. The overall crystallinity of the composite samples was not significantly different from the neat polyamide 12 samples when both sets were allowed to fully anneal. Future work on these systems should involve investigating the cooling rate effects below 20 °C/min. These experiments would give further insight as to how sensitive the size effects of MWNTs are on the crystallization behavior.

Chapter 4

4.1 Chapter 2 Conclusions

Several conclusions can be drawn from the results of the MWNT weight loading studies. The data showed that an increase in the concentration of MWNTs resulted in an increase in the contribution of the γ' -phase peak. All composite samples in these experiments showed an increase in the γ' -phase peak contribution over the neat polyamide 12. This increase was not proportional to the increase in MWNT concentration. These results showed that the MWNTs acted as nucleating agents for the γ' -phase peak. With the γ' -phase having a longer periodicity, it could indicate that the addition of MWNTs to the system is actually disrupting the crystal structure.³⁰

4.2 Chapter 3 Conclusions

The studying of different sizes of MWNTs resulted in some conclusions about the structure of crystallization. At the cooling rate of 10 °C/min, the FWNT sample showed a higher degree of crystallization occurring in the γ' -phase peak while the contribution from the Elicarb and CAER nanotubes samples were not significantly different from each other. All composites in these studies still showed significant increases in γ' -phase peak contribution over the neat polyamide 12. These extra increases in the FWNT composites were not proportional to the amount of MWNTs added indicating that the CAER nanotubes have the best dispersion. In the fully annealed samples, there was no significant change in overall crystallinity between the composites and neat polyamide 12.

4.3 Overall Conclusions

The peak splitting data between the weight loading and nanotube size studies showed that the two behaviors observed can be used together to dictate the desired crystallite structure. Evidence from the annealing conditions indicate that the bonds created between the MWNTs and the polyamide 12 are relatively weak. The annealing phase was able to remove the extra γ' -phase melting peak contribution and resulted in all annealed peaks looking the same. Upon quenching each sample from the melt, the polyamide 12 showed some contribution from the γ' -phase crystallites without the addition of MWNTs. This indicates that polyamide 12 has a degree of polymorphism by itself which has been observed before.^{24-25, 27} However upon adding MWNTs to polyamide 12, an additional increase in the γ' -phase crystallinity could be observed. Combining the data from the two studies done in this thesis indicate that as the diameter of MWNTs decreases and the concentration increases, harsher processing conditions are needed to create homogeneous composites.

The implications of this work can be compiled into Figure 4.1. Figure 4.1 plots the change in the γ' -phase crystallization with the amount of γ' -phase in the neat polyamide 12 subtracted out. This data are from the 10 °C/min cooling rate experiments only but are representative for the other samples. As can be seen, the amount of increased γ' -phase crystallization increases non-linearly with the concentration of MWNTs. From the graph, it appears that the 0.2 wt.% samples are in a linear regime where an increase in MWNT concentration results in a proportional increase in the amount of γ' -phase crystallization. The linear regime could indicate that the MWNT concentration is in a region of isolated small agglomerates. When the concentration is

increased, these agglomerates start interacting with surrounding agglomerates and possibly merge into larger agglomerates. This phenomenon decreases the available surface area available on the MWNTs and reduces their overall effect.

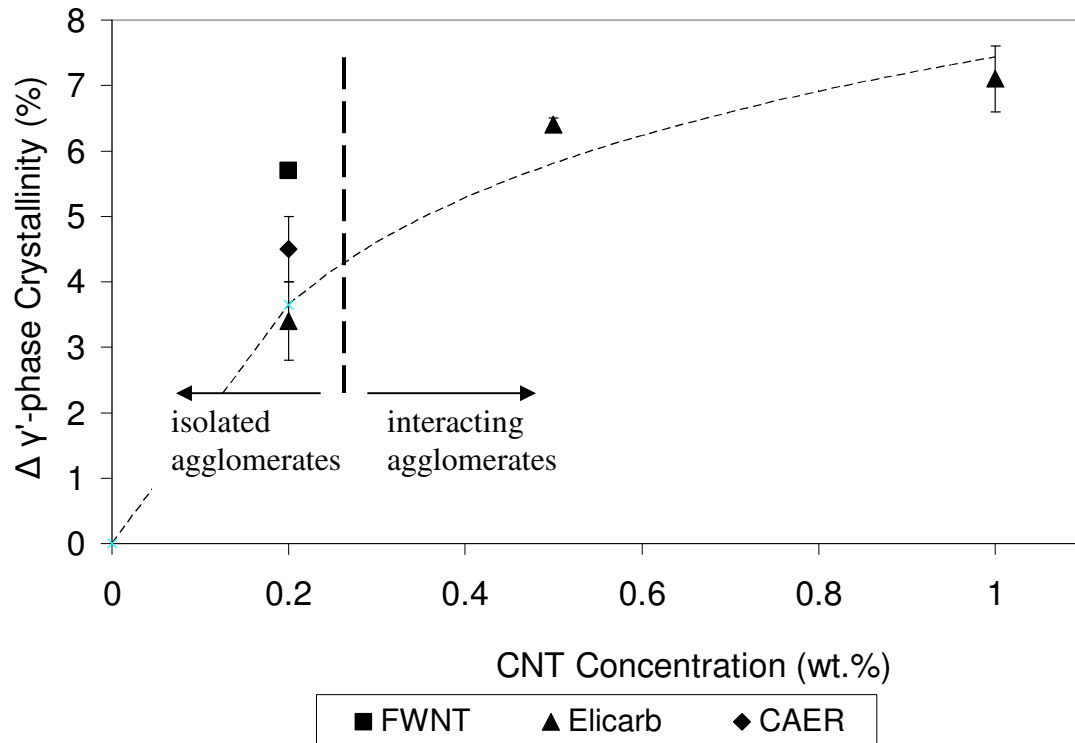


Figure 4.1: A graph showing the increases in γ' -phase crystallinity over the neat polyamide 12 as a function of MWNT concentration. The graph indicates that the 0.2 wt.% MWNT samples are in a linear regime with isolated agglomerates.

4.4 Future Work

There are some future work recommendations for this research. It is recommended that the crystal forms observed in these studies be investigated to confirm the crystal forms present. Researchers have used x-ray diffraction in the past to show the crystal forms explicitly.^{24-25, 27} Further DSC studies are recommended at slower heating

rates to attempt to separate the two peaks further. These studies would help to understand the morphological changes happening in the MWNT composite systems. It would also be recommended that concentrations above 1.0 wt.% and below 0.2 wt.% be mixed to create a comprehensive set of data. This research is a start to understanding the crystallization effects of MWNTs in polyamide 12 and should provide a base for future research.

APPENDIX

Peak Fitting Data

Table A.1: Peak fitting data for the second heating cycle arranged by concentration of MWNTs.

Filler	Cooling Rate	γ' position (°C)	γ' height (W/g)	γ' width (°C)	γ position (°C)	γ height (W/g)	γ width (°C)	R ² Value
Neat	10 °C/min	172.5 ± 0.0	0.50 ± 0.00	1.82 ± 0.02	178.7 ± 0.0	1.05 ± 0.00	1.80 ± 0.07	0.95 ± 0.00
	20 °C/min	172.3 ± 0.2	0.35 ± 0.02	2.00 ± 0.13	179.2 ± 0.2	0.96 ± 0.05	1.94 ± 0.06	0.96 ± 0.01
	30 °C/min	170.8 ± 0.0	0.30 ± 0.01	1.58 ± 0.00	178.7 ± 0.1	1.12 ± 0.02	1.87 ± 0.00	0.92 ± 0.01
	40 °C/min	170.4 ± 0.1	0.21 ± 0.01	1.58 ± 0.00	178.8 ± 0.1	1.18 ± 0.01	1.90 ± 0.03	0.93 ± 0.01
0.2 wt% Elicarb	10 °C/min	175.1 ± 0.1	0.63 ± 0.15	2.16 ± 0.58	178.3 ± 0.1	0.89 ± 0.06	1.75 ± 0.25	0.97 ± 0.01
	20 °C/min	174.6 ± 0.1	0.58 ± 0.05	2.00 ± 0.00	178.9 ± 0.2	0.94 ± 0.02	1.80 ± 0.07	0.97 ± 0.00
	30 °C/min	173.7 ± 0.1	0.56 ± 0.01	2.18 ± 0.06	178.6 ± 0.0	1.00 ± 0.00	1.73 ± 0.00	0.98 ± 0.00
	40 °C/min	173.3 ± 0.2	0.49 ± 0.01	1.87 ± 0.00	178.3 ± 0.1	1.05 ± 0.04	1.82 ± 0.01	0.97 ± 0.00
0.5 wt% Elicarb	10 °C/min	175.7 ± 0.2	0.93 ± 0.00	1.50 ± 0.00	178.2 ± 0.2	0.86 ± 0.01	1.22 ± 0.00	0.95 ± 0.00
	20 °C/min	175.1 ± 0.1	0.54 ± 0.01	2.24 ± 0.00	179.1 ± 0.0	0.86 ± 0.00	1.87 ± 0.00	0.98 ± 0.00
	30 °C/min	175.0 ± 0.0	0.59 ± 0.01	2.29 ± 0.05	179.0 ± 0.1	0.87 ± 0.01	1.66 ± 0.00	0.98 ± 0.00
	40 °C/min	174.5 ± 0.3	0.51 ± 0.03	2.12 ± 0.00	179.0 ± 0.3	0.97 ± 0.05	1.80 ± 0.14	0.97 ± 0.00
1 wt% Elicarb	10 °C/min	176.1 ± 0.2	0.90 ± 0.01	1.62 ± 0.12	178.5 ± 0.4	0.77 ± 0.04	1.18 ± 0.00	0.96 ± 0.00
	20 °C/min	175.4 ± 0.0	0.66 ± 0.01	2.00 ± 0.00	178.6 ± 0.1	0.83 ± 0.01	1.58 ± 0.00	0.97 ± 0.01
	30 °C/min	175.3 ± 0.4	0.60 ± 0.09	2.17 ± 0.17	179.0 ± 0.7	0.86 ± 0.10	1.69 ± 0.19	0.97 ± 0.00
	40 °C/min	174.4 ± 0.0	0.57 ± 0.01	2.14 ± 0.02	178.4 ± 0.0	0.92 ± 0.01	1.65 ± 0.01	0.98 ± 0.01

Table A.2: Peak fitting data for the second heating cycle arranged by size of MWNTs.

Filler	Cooling Rate	γ' position (°C)	γ' height (W/g)	γ' width (°C)	γ position (°C)	γ height (W/g)	γ width (°C)	R ² Value
Neat	10 °C/min	172.5 ± 0.0	0.50 ± 0.00	1.82 ± 0.02	178.7 ± 0.0	1.05 ± 0.00	1.80 ± 0.07	0.95 ± 0.00
	20 °C/min	172.3 ± 0.2	0.35 ± 0.02	2.00 ± 0.13	179.2 ± 0.2	0.96 ± 0.05	1.94 ± 0.06	0.96 ± 0.01
	30 °C/min	170.8 ± 0.0	0.30 ± 0.01	1.58 ± 0.00	178.7 ± 0.1	1.12 ± 0.02	1.87 ± 0.00	0.92 ± 0.01
	40 °C/min	170.4 ± 0.1	0.21 ± 0.01	1.58 ± 0.00	178.8 ± 0.1	1.18 ± 0.01	1.90 ± 0.03	0.93 ± 0.01
0.2 wt% FWNT	10 °C/min	175.3 ± 0.1	0.80 ± 0.03	1.84 ± 0.00	178.5 ± 0.1	0.86 ± 0.05	1.41 ± 0.00	0.97 ± 0.01
	20 °C/min	174.6 ± 0.0	0.52 ± 0.08	1.94 ± 0.06	178.9 ± 0.3	0.88 ± 0.05	1.93 ± 0.19	0.97 ± 0.00
	30 °C/min	173.5 ± 0.1	0.52 ± 0.01	2.00 ± 0.00	178.6 ± 0.0	0.98 ± 0.01	1.90 ± 0.03	0.96 ± 0.01
	40 °C/min	172.9 ± 0.3	0.45 ± 0.02	1.98 ± 0.25	178.6 ± 0.1	1.06 ± 0.06	1.87 ± 0.13	0.97 ± 0.02
0.2 wt% Elicarb	10 °C/min	175.1 ± 0.1	0.63 ± 0.15	2.16 ± 0.58	178.3 ± 0.1	0.89 ± 0.06	1.75 ± 0.25	0.97 ± 0.01
	20 °C/min	174.6 ± 0.1	0.58 ± 0.05	2.00 ± 0.00	178.9 ± 0.2	0.94 ± 0.02	1.80 ± 0.07	0.97 ± 0.00
	30 °C/min	173.7 ± 0.1	0.56 ± 0.01	2.18 ± 0.06	178.6 ± 0.0	1.00 ± 0.00	1.73 ± 0.00	0.98 ± 0.00
	40 °C/min	173.3 ± 0.2	0.49 ± 0.01	1.87 ± 0.00	178.3 ± 0.1	1.05 ± 0.04	1.82 ± 0.01	0.97 ± 0.00
0.2 wt% CAER	10 °C/min	175.4 ± 0.0	0.75 ± 0.06	1.84 ± 0.00	179.0 ± 0.0	0.92 ± 0.02	1.63 ± 0.03	0.97 ± 0.01
	20 °C/min	174.4 ± 0.0	0.50 ± 0.01	2.00 ± 0.00	179.0 ± 0.1	0.90 ± 0.02	2.06 ± 0.06	0.97 ± 0.00
	30 °C/min	173.3 ± 0.1	0.52 ± 0.02	2.05 ± 0.18	178.5 ± 0.1	1.02 ± 0.01	1.83 ± 0.10	0.96 ± 0.02
	40 °C/min	172.6 ± 0.0	0.50 ± 0.00	1.82 ± 0.02	178.2 ± 0.0	1.15 ± 0.01	1.60 ± 0.00	0.96 ± 0.00

References

1. Zhang, W. D.; Shen, L.; Phang, I. Y.; Liu, T., Carbon nanotubes reinforced nylon-6 composite prepared by simple melt-compounding. *Macromolecules* **2004**, *37* (2), 256-259.
2. Andrews, R.; Jacques, D.; Minot, M.; Rantell, T., Fabrication of carbon multiwall nanotube/polymer composites by shear mixing. *Macromolecular Materials and Engineering* **2002**, *287* (6), 395-403.
3. Winey, K. I.; Vaia, R. A., Polymer nanocomposites. *MRS Bulletin* **2007**, *32* (4), 314-319.
4. Zhang, S.; Minus, M. L.; Zhu, L. B.; Wong, C. P.; Kumar, S., Polymer transcrystallinity induced by carbon nanotubes. *Polymer* **2008**, *49* (5), 1356-1364.
5. Broadbelt, L. J.; Klein, M. T.; Dean, B. D.; Andrews, S. M., Thermal-degradation of aliphatic-aromatic polyamides - kinetics of N,N'-dihexylisophthalamide neat and in presence of copper iodide. *Journal of Applied Polymer Science* **1995**, *56* (7), 803-815; Rangari, V. K.; Yousuf, M.; Jeelani, S.; Pulikkathara, M. X.; Khabashesku, V. N., Alignment of carbon nanotubes and reinforcing effects in nylon-6 polymer composite fibers. *Nanotechnology* **2008**, *19* (24), 245703.
6. Iijima, S., Helical microtubules of graphitic carbon. *Nature* **1991**, *354* (6348), 56-58.
7. Treacy, M. M. J.; Ebbesen, T. W.; Gibson, J. M., Exceptionally high Young's modulus observed for individual carbon nanotubes. *Nature* **1996**, *381* (6584), 678-680.
8. Ebbesen, T. W.; Lezec, H. J.; Hiura, H.; Bennett, J. W.; Ghaemi, H. F.; Thio, T., Electrical conductivity of individual carbon nanotubes. *Nature* **1996**, *382* (6586), 54-56; Chiu, H. Y.; Deshpande, V. V.; Postma, H. W. C.; Lau, C. N.; Miko, C.; Forro, L.; Bockrath, M., Ballistic phonon thermal transport in multiwalled carbon nanotubes. *Physical Review Letters* **2005**, *95* (22), 226101.
9. Yu, M. F.; Lourie, O.; Dyer, M. J.; Moloni, K.; Kelly, T. F.; Ruoff, R. S., Strength and breaking mechanism of multiwalled carbon nanotubes under tensile load. *Science* **2000**, *287* (5453), 637-640; Ding, W.; Calabri, L.; Kohlhaas, K. M.; Chen, X.; Dikin, D. A.; Ruoff, R. S., Modulus, fracture strength, and brittle vs. plastic response of the outer shell of arc-grown multi-walled carbon nanotubes. *Experimental Mechanics* **2007**, *47* (1), 25-36.
10. He, L. H.; Xu, Q.; Hue, C. W.; Song, R., Effect of Multi-Walled Carbon Nanotubes on Crystallization, Thermal, and Mechanical Properties of Poly(vinylidene fluoride). *Polymer Composites* **2010**, *31* (5), 921-927.

11. Razavi-Nouri, M.; Ghorbanzadeh-Ahangari, M.; Fereidoon, A.; Jahanshahi, M., Effect of carbon nanotubes content on crystallization kinetics and morphology of polypropylene. *Polymer Testing* **2009**, *28* (1), 46-52.
12. Minus, M. L.; Chae, H. G.; Kumar, S., Single wall carbon nanotube templated oriented crystallization of poly(vinyl alcohol). *Polymer* **2006**, *47* (11), 3705-3710.
13. Zhang, W.; Picu, R. C.; Koratkar, N., The effect of carbon nanotube dimensions and dispersion on the fatigue behavior of epoxy nanocomposites. *Nanotechnology* **2008**, *19* (28).
14. Giraldo, L. F.; Lopez, B. L.; Brostow, W., Effect of the type of carbon nanotubes on tribological properties of polyamide 6. *Polymer Engineering and Science* **2009**, *49* (5), 896-902.
15. Eitan, A.; Fisher, F. T.; Andrews, R.; Brinson, L. C.; Schadler, L. S., Reinforcement mechanisms in MWCNT-filled polycarbonate. *Composites Science and Technology* **2006**, *66* (9), 1162-1173.
16. Liu, T. X.; Phang, I. Y.; Shen, L.; Chow, S. Y.; Zhang, W. D., Morphology and mechanical properties of multiwalled carbon nanotubes reinforced nylon-6 composites. *Macromolecules* **2004**, *37* (19), 7214-7222.
17. Chavarria, F.; Paul, D. R., Comparison of nanocomposites based on nylon 6 and nylon 66. *Polymer* **2004**, *45* (25), 8501-8515.
18. Krause, B.; Potschke, P.; Haussler, L., Influence of small scale melt mixing conditions on electrical resistivity of carbon nanotube-polyamide composites. *Composites Science and Technology* **2009**, *69*, 1505-1515.
19. Wu, T. M.; Liao, C. S., Polymorphism in nylon 6/clay nanocomposites. *Macromolecular Chemistry and Physics* **2000**, *201* (18), 2820-2825.
20. Lu, H. M.; Xu, X. M.; Li, X. H.; Zhang, Z. J., Morphology, crystallization and dynamic mechanical properties of PA66/nano-SiO₂ composites. *Bulletin of Materials Science* **2006**, *29* (5), 485-490.
21. Aharoni, S. M., *n-Nylons: Their synthesis, structure and properties*. John Wiley & Sons Ltd: Chichester, 1997.
22. Sandler, J. K. W.; Pegel, S.; Cadek, M.; Gojny, F.; van Es, M.; Lohmar, J.; Blau, W. J.; Schulte, K.; Windle, A. H.; Shaffer, M. S. P., A comparative study of melt spun polyamide-12 fibres reinforced with carbon nanotubes and nanofibres. *Polymer* **2004**, *45* (6), 2001-2015.
23. Zhang, Y.; Yang, J. H.; Ellis, T. S.; Shi, J., Crystal structures and their effects on the properties of polyamide 12/clay and polyamide 6-polyamide 66/clay nanocomposites. *Journal of Applied Polymer Science* **2006**, *100* (6), 4782-4794.

24. Li, L. B.; Koch, M. H. J.; de Jeu, W. H., Crystalline structure and morphology in nylon-12: A small- and wide-angle X-ray scattering study. *Macromolecules* **2003**, *36* (5), 1626-1632.
25. Ramesh, C., Crystalline transitions in nylon 12. *Macromolecules* **1999**, *32* (17), 5704-5706.
26. Mathias, L. J.; Johnson, C. G., Solid-state NMR investigation of nylon-12. *Macromolecules* **1991**, *24* (23), 6114-6122.
27. Northolt, M. G.; Vanaarts.Jj; Tabor, B. J., Polymorphism in nylon-12. *Journal of Polymer Science Part a-2-Polymer Physics* **1972**, *10* (1), 191-192.
28. Wang, D. L.; Shao, C. G.; Zhao, B. J.; Bai, L. G.; Wang, X.; Yan, T. Z.; Li, J. J.; Pan, G. Q.; Li, L. B., Deformation-induced phase transitions of polyamide 12 at different temperatures: An in situ wide-angle X-ray scattering study. *Macromolecules* **2010**, *43* (5), 2406-2412.
29. Ishikawa, T.; Nagai, S.; Kasai, N., Thermal-behavior of alpha-nylon-12. *Journal of Polymer Science Part B-Polymer Physics* **1980**, *18* (6), 1413-1419.
30. Hiramatsu, N.; Haraguchi, K.; Hirakawa, S., Study of transformations among alpha,gamma and gamma' forms in nylon 12 by x-ray and DSC. *Japanese Journal of Applied Physics Part 1-Regular Papers Short Notes & Review Papers* **1983**, *22* (2), 335-339.